



HAL
open science

Unified approach for extrapolation and bridging of adult information in early-phase dose-finding paediatric studies

Caroline Petit, Adeline Samson, Satoshi Morita, Moreno Ursino, Vincent Jullien, Emmanuelle Comets, Sarah Zohar

► To cite this version:

Caroline Petit, Adeline Samson, Satoshi Morita, Moreno Ursino, Vincent Jullien, et al.. Unified approach for extrapolation and bridging of adult information in early-phase dose-finding paediatric studies. *Statistical Methods in Medical Research*, 2018, 27 (6), pp.1860-1877. 10.1177/0962280216671348 . hal-01623760

HAL Id: hal-01623760

<https://hal.science/hal-01623760>

Submitted on 25 Oct 2017

HAL is a multi-disciplinary open access archive for the deposit and dissemination of scientific research documents, whether they are published or not. The documents may come from teaching and research institutions in France or abroad, or from public or private research centers.

L'archive ouverte pluridisciplinaire **HAL**, est destinée au dépôt et à la diffusion de documents scientifiques de niveau recherche, publiés ou non, émanant des établissements d'enseignement et de recherche français ou étrangers, des laboratoires publics ou privés.

Unified approach for extrapolation and bridging of adult information in early-phase dose-finding paediatric studies

Journal Title

XX(X):2–30

© The Author(s) 0000

Reprints and permission:

sagepub.co.uk/journalsPermissions.nav

DOI: 10.1177/ToBeAssigned

www.sagepub.com/

² Caroline PETIT ¹, Adeline SAMSON ², Satoshi MORITA ³, Moreno URSINO ¹, Jérémié
³ GUEDJ ⁴, Vincent JULLIEN ⁵, Emmanuelle COMETS ^{4,6}, Sarah ZOHAR ¹

Abstract

The number of trials conducted, and the number of patients per trial are typically small in paediatric clinical studies. This is due to ethical constraints and the complexity of the medical process for treating children. While incorporating prior knowledge from adults may be extremely valuable, this must be done carefully. In this paper, we propose a unified method for designing and analysing dose-finding trials in paediatrics, while bridging information from adults. The dose-range is calculated under three extrapolation options, linear,
⁴ allometry and maturation adjustment, using adult pharmacokinetic data. To do this, it is assumed that target exposures are the same in both populations. The working model and prior distribution parameters of the dose-toxicity and dose-efficacy relationships are obtained using early-phase adult toxicity and efficacy data at several dose levels. Priors are integrated into the dose-finding process through Bayesian model selection or adaptive priors. This calibrates the model to adjust for misspecification if the adult and pediatric data are very different. We performed a simulation study which indicates that incorporating prior adult information in this way may improve dose selection in children.

Keywords

dose-finding, bridging, extrapolation, adults observations, paediatrics trials, bayesian inference

1 Introduction

Phase I dose-finding studies represent the first transition from laboratory work to a clinical setting and aim to obtain reliable information on the pharmacokinetics (PK), safety and tolerability of a drug. Typically, these trials are performed on healthy subjects unless the drug is intended for the treatment of malignancies (i.e., oncology).

In paediatric clinical trials, invasive procedures are avoided or at least minimised for ethical reasons and the usefulness of clinical trials in children has been widely debated over the last decades¹, as highlighted by two papers recently published in the journal of the American Academy for Paediatrics^{2,3}. Several authors and specialists have reported a critical need for more clinical studies in paediatrics combined with an improvement in the methodologies used in practice. Some authors have argued that incorporating prior knowledge from adults should help attain a better understanding of the paediatric population. However, other studies have shown that children should not be considered small adults but rather a specific population with a different metabolism that is not necessarily linearly related to growth^{1,4}.

¹INSERM, UMRS 1138, CRC, Team 22, Univ. Paris 5, Univ. Paris 6, Paris, France.

²LJK, UMR CNRS 5224, Univ. Grenoble Alpes, Grenoble, France.

³Department of Biomedical Statistics and Bioinformatics, Kyoto University Graduate School of Medicine, 54 Kawahara-cho, Shogoin, Sakyo-ku, Kyoto 606-8507, Japan.

⁴INSERM, IAME, UMR 1137, F-75018 Paris, France; Univ Paris Diderot, Sorbonne Paris Cité, F-75018 Paris, France.

⁵Pharmacology Department, Univ. Paris 5, Sorbonne Paris Cité, Inserm U1129, HEGP, Paris, France.

⁶INSERM, CIC 1414, Univ. Rennes 1, Rennes, France.

Corresponding author:

Sarah Zohar
INSERM UMRS 1138
Centre de Recherche des Cordeliers,
Escalier D, 1er étage
15 rue de l'école de médecine
75006 Paris
Email: sarah.zohar@inserm.fr

19 For dose-finding paediatric studies, guidelines have been suggested for the choice of starting subset doses⁶
20 (e.g., the starting dose should equal 80% of the adult recommended dose, and these doses should then
21 be increased by 30% to obtain the subset doses). However, these recommendations are arbitrary and
22 do not rely on any scientific justifications. As a result, to improve the selection of the dose-range that
23 should be used in a paediatric study based on the use of adult information, this information should be
24 investigated through (1) the choice of the dose-range for a paediatric trial, (2) the dose-finding model and
25 (3) its parametrisation.

26 **Motivating example:** Erlotinib is an oral inhibitor of the epidermal growth factor receptor (EGFR)
27 tyrosine kinase that blocks cell cycle progression and can slow down tumour progression. This anticancer
28 agent was approved by the Food and Drug Administration (FDA) for the treatment of glioblastoma in
29 adults. Several early-phase trials were conducted in adults to study the toxicity and PK of this drug at
30 different dose levels⁷⁻¹³, and two phase I paediatric studies were conducted after the publication of the
31 results in adults. However, only a small amount of the knowledge obtained from the adult trials was used in
32 the design and planning of the paediatric trials. Georger *et al.*¹⁴ used 80% of the dose recommended for
33 adults as the starting dose and incremented this dose by steps of 25 mg/m² to obtain the subset dose levels;
34 however, these researchers provided no scientific justifications for these choices. Neither the available
35 adult information nor expert opinions were used to parametrise the model-based dose-finding design.
36 Jakacki *et al.*¹⁵ also conducted a phase I dose-finding trial for erlotinib in paediatric subjects and selected
37 the starting dose level according to the bioavailability of the solution for injection. The authors did not
38 describe the method used for the selection of the subset dose levels, and information from studies on
39 the adult population was not used to build a more appropriate trial for the paediatric population. This
40 motivating example highlights the need for the development of proper extrapolation or bridging methods
41 that should be used when prior knowledge from the adult population is available.

42 In the development of a dose-finding model for the paediatric population, difficulties regarding the
43 evaluation of toxicity alone (except in oncology) have led to the use of a joint model for both toxicity
44 and efficacy instead of a model that evaluates toxicity prior to efficacy. Several statistical methods are

45 available for the design of early stage phase I/II clinical trials. Among them, Bayesian methods, such as
46 the EFFTOX design and the bivariate Continual Reassessment Method (bCRM), have been proposed^{16;17}.
47 Although initially used in oncology settings, these methods have also been used for studies of the paediatric
48 population¹⁸. Additionally, Broglio *et al.*¹⁹ proposed a method in which adult and paediatric trials are
49 performed simultaneously with dose-finding models for each population that share an identical slope but a
50 different intercept. Doussau *et al.*⁶ reviewed the methods that could also be used in paediatrics, such as
51 '3+3', CRM with its modifications and EWOC.

52 The use of an adaptive dose-finding method requires that **three** components be fixed prior to initiation of
53 the trial:

54 (1) **Dose-range**: Misspecification of the dose-range in a clinical trial can lead to inappropriate dose
55 selection and invalidation of the trial. Because children have a specific metabolism, we proposed the
56 establishment of a dose-range that is more suitable to the paediatric metabolism⁵. For that purpose, we
57 proposed the estimation of paediatric PK parameters from adult PK data, which are often available long
58 before data for the paediatric population are available, using extrapolation techniques, such as allometry
59 and maturation.

60 (2) **Working model (WM)** or initial guess of dose-toxicity and dose-efficacy relationships: Working
61 models are usually selected based on information from experts. In some cases, a unique choice of WM
62 can be misleading and result in the selection of an inappropriate dose. One approach for overcoming this
63 issue is to use several WMs for toxicity and efficacy using the bCRM^{20;21} and to select the best model
64 with based on the Watanabe-Akaike information criteria developed by Watanabe (WAIC)^{22;23}.

65 (3) **Prior distribution** of the model parameter(s) to be estimated: Although using standard non-informative
66 priors is often advised, it is difficult to assess to what degree this choice is informative or non-informative.
67 Moreover, it may be interesting to include information in the priors while controlling the informativeness
68 in cases with a small effective sample size, particularly in paediatrics. Regarding the selection of priors,
69 we considered a method developed by S. Morita^{24;25}, which consists of evaluating the informativeness of
70 a prior in terms of the effective sample size. The more informative a prior is, the more patients are needed

71 to compensate for it. In a paediatric setting, where the sample size is small, this scale is a strong asset for
72 evaluating a chosen prior. However, if the chosen prior is too informative or misspecified compared with
73 the paediatric reality, a non-informative alternative should be available. In this case, we have modified
74 a method proposed by Lee *et al.* and Zhang *et al.*^{26:27} that introduced the concept of "adaptive-prior"
75 into dose-finding studies. The idea is to be able to switch during the trial to a less informative prior if a
76 misspecification in the prior choice is detected.

77 The aim of this paper is to propose a unified approach for the design of a paediatric dose-finding clinical
78 trial through the extrapolation and bridging of information gleaned from the adult population. We have
79 gathered and modified various methods that have been developed in different fields to propose a unified
80 approach. The novelty of our work consists of the proposal of extrapolation with maturation from adult PK
81 into the definition of the dose-range (1) and of the use of adult information from several sources to better
82 parameterise the dose-finding design (2)-(3) instead of leaving these decisions to arbitrary choices. In this
83 work, several options are proposed for the selection of the dose-range, the WM and/or the parametrisation
84 of the dose-finding design (Figure 1). Section 2 details the dose-finding model, illustrates the options for
85 specifying the dose-range and describes the parametrisation of the design using adult information. The
86 simulation settings and results are given in Sections 3 and 4. Finally, guidelines are proposed in Section 5
87 and, a discussion is provided in Section 6.

88 **2 Model and methods**

89 We considered the design of a phase I/II clinical trial in the paediatric population using the Bayesian bCRM
90 as the dose allocation method. Section 2.1 presents the bCRM method and the dose allocation algorithm.
91 The first step (1) consists of defining the doses to evaluate. We proposed three options for the selection of
92 the dose-range using adult to paediatric extrapolation methods, which use different adjustments of the
93 paediatric dose from the adult's recommended dose: linear, related to weight with allometry, and related to
94 physiological processes with maturation functions to account for maturation differences between adults
95 and children. These three options are described in Section 2.2.1. Once the doses are defined, step (2)

consists of associating each dose with a given initial guess of the toxicity and efficacy probability, and these relationships are called "working models" (WMs). The selected doses are supposed to be within a desirable toxicity and efficacy interval to ensure that patients are not overtreated or undertreated. The WMs are constructed by gathering several prior sources of information from the adult population, such as pharmacokinetics, phase I trials, phase II trials, toxicity and clinical response. We proposed two options for the WMs: using only one WM, or using several WMs and selecting the optimal WM using automatic criteria. A description of the methods used to elaborate the WMs is given in Section 2.2.2. Finally, step (3) involves the selection of the dose-response parameter density of the priors used in the bCRM. We proposed two options for these priors: considering adult information or considering the case with the least information. These are described in Section 2.2.3, and a summary of this general framework is presented in Figure 1.

[Figure 1 about here.]

2.1 Bivariate Continual Reassessment Method (bCRM)

In this general framework, we used the bivariate continual reassessment method (bCRM) as phase I/II dose-finding methods. This design proposes a joint model for both toxicity and efficacy^{17;28}. The aim of this method is to identify the safe most successful dose (sMSD) which is the most successful dose under toxicity restriction. Let $d_1 < d_2 < \dots < d_K$ be the paediatric doses to be evaluated in the study, with K the number of discrete dose levels, and n the total number of patients to be recruited. Choice of doses is discussed in Section 2.2.1. Toxicity and efficacy are random binary variables (0,1) where $Y_j = 1$ denotes a toxicity for patient j ($j \in 1, \dots, n$) and $V_j = 1$ denotes a positive response. The dose level X_j is a random variable taking discrete values x_j , where $x_j \in \{d_1, \dots, d_K\}$. The probability of toxicity at dose level $X_j = x_j$ is given by $R(x_j) = \Pr(Y_j = 1 | X_j = x_j)$, the probability of efficacy with no toxicity at dose level $X_j = x_j$ is given by $Q(x_j) = \Pr(V_j = 1 | X_j = x_j, Y_j = 0)$ and the overall success is obtained by $P(d_i) = Q(d_i)\{1 - R(d_i)\}$.

120 Following the under-parametrised model approximation proposed by O'Quigley *et al.*²⁸, we have
 121 $R(d_i) = \Psi(d_i, a) = \alpha_i^{\exp(a)}$ and $Q(d_i) = \Phi(d_i, b) = \beta_i^{\exp(b)}$ where $R(d_i)$ and $Q(d_i)$ are monotonic and
 122 increasing with dose, $a \in \mathbb{R}$ (resp. $b \in \mathbb{R}$). Parameters $0 < \alpha_1 < \dots < \alpha_K < 1$ (resp. $0 < \beta_1 < \dots < \beta_K < 1$)
 123 correspond to the working models (WM) to be chosen by the user (see Section 2.2.2). The joint probability
 124 density function is defined by:

$$f(y, v; d_i, a, b) = \Psi(d_i, a)^y (1 - \Psi(d_i, a))^{(1-y)} \Phi(d_i, b)^v (1 - \Phi(d_i, b))^{(1-v)}. \quad (1)$$

125 Under Bayesian inference, the prior distributions for a and b are respectively denoted by $\pi(a)$ and $\pi(b)$.
 126 Choice of the priors is discussed in Section 2.2.3.

127 The dose allocation rule is the following. Let us denote \hat{a} and \hat{b} the estimated means of the posterior
 128 distribution of a given WM for the current available data of toxicity and efficacy already observed with the
 129 included patients. The estimated probability of toxicity is $\hat{R}(d_i) \cong \Psi(d_i, \hat{a})$ and the efficacy $\hat{Q}(d_i) \cong \Phi(d_i, \hat{b})$.
 130 Finally, the overall probability of success is given by $\hat{P}(d_i) = (1 - \hat{R}(d_i))\hat{Q}(d_i)$. The recommended dose
 131 for the new next cohort of patients is the sMSD d^* that is the dose maximising $\hat{P}(d_1), \hat{P}(d_2), \dots, \hat{P}(d_K)$
 132 under a constraint of toxicity target, defined with parameter τ , such that $\hat{R}(d^*) \leq \tau$.

133 **In practice:** For escalation, dose skipping was allowed only on doses already tested. A start-up phase was
 134 implemented to gather data before estimating the model parameters. The first cohort of three patients were
 135 treated at a specified dose x_0 . If no toxicity was observed, a new cohort of three patients would be included
 136 at the direct higher dose. This process was repeated until at least a toxicity was observed or all doses
 137 were tested. We then moved to the dose-finding algorithm using bCRM. For safety reason, a stopping-rule
 138 was added to our algorithm, that is, if $\Pr(\Psi(d_1, a) > \tau) > 0.9$, the trial was terminated. At the opposite,
 139 a second stopping rule was defined in case of non-efficacy. For a threshold of minimum efficacy τ' , if
 140 $\Pr(\Phi(d_K, b) < \tau') > 0.9$ the trial was terminated.

2.2 Extrapolation from adult data to paediatrics

Similarly to any model-based phase I/II dose-finding method, the design can be sensitive to three settings: (1) the choice of dose-range, (2) the WMs and (3) the prior distributions. In our proposed method, we suggest that these settings be based on extrapolations from the adult to paediatric population.

2.2.1 Specification of a dose-range Paediatric data are often rare, and paediatric doses are usually selected based on existing recommendations for adult doses. We proposed three options for the selection of paediatric doses: linear and allometric extrapolation from adult doses, which are the current practices, and use of maturation, which is a novel approach in this context.

Option linear adjustment (LA). Using the adult dose $d_{ad,i}$ ($i = 1, \dots, K$), weight W_{ch} of children and average weight W_{ad} of adults, the linear adjustment (LA) option consists of defining the paediatric dose d_i as

$$d_i = d_{ad,i} \times \frac{W_{ch}}{W_{ad}}. \quad (2)$$

Option allometry adjustment (AA). This option introduces a scale parameter describing the rate at which the weight increases, which is usually equal to 0.75⁵:

$$d_i = d_{ad,i} \times \left(\frac{W_{ch}}{W_{ad}} \right)^{0.75}. \quad (3)$$

Option maturation adjustment (MA). The use of maturation functions allows the adjustments to better reflect the paediatric physiology⁴. We took advantage of this allometry-maturation approach²⁹ to propose a paediatric dose-range calculation, denoted maturation adjustment (MA). Our method is based on the available adult PK knowledge. For a given adult dose $d_{ad,i}$, the corresponding children's dose d_i was defined such that the same exposure to the dose was achieved. This exposure can be quantified by the AUC or C_{max} , which depends on PK parameters (typically clearance). Let Cl_{ch} (resp. Cl_{ad}) be the paediatric (resp. adult) clearance, and $AUC(d, Cl) = d/Cl$ be the corresponding AUC . The goal of achieving equal

161 exposure in adults and children leads to the following definition for the paediatric dose $d_i = d_{ad,i} \times \frac{Cl_{ch}}{Cl_{ad}}$.
 162 If the adult PK clearance is available from previously published PK studies, the paediatric clearance is
 163 generally unknown but might be extrapolated through allometry and maturation functions. The resulting
 164 general equation defining the evolution of clearance in children according to age and weight for a specific
 165 drug is

$$\frac{Cl_{ch}}{F_{ch}} = Cl_{ad} \times \underbrace{\sum_h \%CYP_h MAT_{CYP_h}(AGE)}_{\text{Clearance maturation}} \times \underbrace{\frac{F}{F_{ch}}}_{\text{Bioavailability maturation}} \times \underbrace{\left(\frac{W_{ch}}{W_{ad}}\right)^{0.75}}_{\text{Allometry}} \quad (4)$$

166 Using allometry to account for size, the bioavailability and clearance sections of the equation account
 167 for the maturation process in the paediatric population^{4;29}. The maturation of clearance depends on
 168 cytochromes (CYPs), which are responsible for the hepatic elimination process. In Eq. 4, $\%CYP_h$ is the
 169 proportion of the hepatic metabolism for hepatic CYP and MAT_{CYP_h} , which is the maturation function
 170 related to age. The maturation functions for each CYP can be developed empirically or obtained from
 171 the literature (in particular, see Johnson *et al.*⁵). Bioavailability is defined as the fraction of the dose
 172 (bioavailable fraction) that reaches the systemic circulation after oral administration. Indeed, only a
 173 fraction of the dose is absorbed at the gut level, and this fraction is defined as f_{abs} . Before reaching
 174 the systemic circulation, the drug undergo a first pass effect in the gut and subsequently a second pass
 175 effect in the liver due to the presence of CYPs. These pass effects are characterised by the gut extraction
 176 coefficient E_G and the hepatic extraction coefficient E_H , respectively. The bioavailability in adults equals
 177 $F = f_{abs}(1 - E_G)(1 - E_H)$. In the paediatric population, the amount of CYPs in the gut and liver might not
 178 have reached the adult amount, and this process depends on age. Therefore, the bioavailability in children
 179 F_{ch} can be expressed as

$$F_{ch} = f_{abs}(1 - E_G \times \sum_g \%CYP_g MAT_{CYP_g}(AGE))(1 - E_H \sum_h \%CYP_h MAT_{CYP_h}(AGE)) \quad (5)$$

180 where $\%CYP_g$ and MAT_{CYP_g} are similar to the above-described functions but applied to the gut. Using
 181 $\frac{Cl_{ch}}{Cl_{ad}}$, this approach yields the following paediatric dose:

$$d_i = d_{ad,i} \times \sum_h \%CYP_h MAT_{CYP_h}(AGE) \times \frac{F}{F_{ch}} \times \left(\frac{W_{ch}}{W_{ad}} \right)^{0.75} \quad (6)$$

182
 183 The three above-described options were compared by building a dose-range for LA, AA and MA. The
 184 adult average weight W_{ad} was considered to equal 70 kg, and the average paediatric weight is not
 185 properly defined. A population of $N = 100,000$ patients aged 0 to 21 years was then simulated using P³M
 186 software^{30;31} and for each simulated subject, the individual clearance $Cl_{ch,j}$ ($j = 1, \dots, N$) was calculated.
 187 In addition, for each option (LA, AA and MA) and for all individuals $j = 1, \dots, N$, a set of doses $d_{i,j}$,
 188 $i = 1, \dots, K$, expressed in mg/kg, were computed. For a given age group, the i^{th} dose was obtained by
 189 averaging the mean across all patients belonging to that age group and rounding up to the closest multiple
 190 of 5 (due to practice constraints).

191 *2.2.2 Choice of working models using adult information* After selecting the dose-range for the study,
 192 the next step is to parametrise the model-based dose-finding method, i.e., the bCRM. In this method, the
 193 WMs α_i and β_i , $i = 1, \dots, K$ have to be chosen carefully. We proposed two options: defining a unique
 194 WM (WM1-bCRM), and defining several WMs (WAIC-bCRM) and selecting the best one using an
 195 automatic criteria. The methodology used to build a WM for both options follows three stages. First, the
 196 toxicity probabilities are calculated based on adult PK information. We denoted $\gamma_\ell^{(1)}$ as the corresponding
 197 probability of toxicity for the adult doses $d_{ad,\ell}$, $\ell = 1, \dots, L$ tested in clinical trials. Assuming equal
 198 exposure in adults and children, this approach yielded estimated toxicities $\gamma_\ell^{(1)}$ for the children's doses
 199 d_ℓ , $\ell = 1, \dots, L$. Note that these doses are not necessarily concordant with the dose-range in the paediatric
 200 population. Indeed, the doses tested in clinical trials $d_{ad,\ell}$ may be different from the adult doses selected to
 201 establish the paediatric dose-range. Second, information from toxicity studies (phase I and I/II clinical
 202 trials) is gathered using a retrospective design of pooled data³². Details on this method can be found in

203 Appendix A. Through simulation and a power model with re-estimated parameters, the results were pooled
 204 using a down-weighting method, yielding a second estimate $\gamma_\ell^{(2)}$ of the probabilities of toxicities for the
 205 adult doses $d_{ad,\ell}$, or the equivalent children's doses d_ℓ was available. The third step consists of defining a
 206 mixture estimator of the toxicity probabilities $\gamma_\ell^{(T)} = \lambda_\ell \gamma_\ell^{(1)} + (1 - \lambda_\ell) \gamma_\ell^{(2)}$, where λ_ℓ is a weight selected
 207 through a data-driven approach as defined by Liu *et al.*²⁰ using data collected from adult clinical trials.
 208 The weights were defined as $\lambda_\ell = LR_\ell / (LR_\ell + 1)$ where LR_ℓ is the estimated likelihood ratio between the
 209 two estimated models for a dose level ℓ :

$$LR_\ell = \frac{\gamma_\ell^{(1) n_{\ell,tox} (1 - \gamma_\ell^{(1)})^{(n_\ell - n_{\ell,tox})}}{\gamma_\ell^{(2) n_{\ell,tox} (1 - \gamma_\ell^{(2)})^{(n_\ell - n_{\ell,tox})}}$$

210 where $n_{\ell,tox}$ is the overall number of toxicities and n_ℓ is the number of patients given dose ℓ . Finally,
 211 if the doses $d_\ell, \ell = 1, \dots, L$ obtained through adult information did not match the paediatric dose-range
 212 $\{d_1, \dots, d_K\}$ found as described in the previous section, a logit curve is fit to $(d_\ell, \gamma_\ell^{(T)})$ to obtain a curve
 213 $\eta(d)$ of the probability of toxicity, which allows the calculation of the probability of toxicity for the
 214 paediatric doses d_j .

215 We now describe in detail the two proposed options.

216 **Option unique WM (WM1-bCRM).** We proposed the use of a unique WM extracted from the available
 217 adult information:

$$\text{WM1 : } \alpha_i = \eta(d_i) \text{ for } i = 1, \dots, K \quad (7)$$

218 **Option WAIC (WAIC-bCRM).** To reduce the arbitrariness of a unique choice of WM $\alpha_i, i = 1, \dots, K$, we
 219 proposed the definition of several WMs followed by model selection. Following Liu *et al.*, two additional
 220 WMs were built from the above-mentioned WM obtained as follows:

$$\begin{aligned} \text{WM2 : } \alpha_i &= \eta(d_{i+1}) \text{ for } i = 1, \dots, K - 1 \text{ and } \alpha_K = \frac{\eta(d_K) + 1}{2} \\ \text{WM3 : } \alpha_1 &= \frac{\eta(d_1)}{2} \text{ and } \alpha_i = \eta(d_{i-1}) \text{ for } i = 2, \dots, K \end{aligned} \quad (8)$$

221 The bCRM was performed for the **three** working models, **and** model selection was based on the Watanabe-
 222 Akaike information criteria (WAIC) ^{22;23} **was applied**. This approach selected the WM that best fit the
 223 data and returned an estimate of parameters a and b for each dose i .

224 **2.2.3 Specification of prior density** In addition to the WMs, when using Bayesian model-based methods,
 225 the prior density of the dose-response model needs to be specified. In our framework, the prior distributions
 226 of the dose-toxicity model parameters were selected using two different parametrisations based on either
 227 (i) the adult information (option ESS, AP_{ESS}-bCRM) or (ii) least information (option Least informative
 228 prior, AP_{LIP}-bCRM). In the first option, due to the sparsity of the data, it appears appropriate to attempt to
 229 incorporate observations into the prior. However, the information introduced by the prior distributions to
 230 the posterior should not overtake the information introduced by the likelihood distribution.

231 **Option ESS (AP_{ESS}-bCRM).** Let $\pi_{ESS}(a)$ be the prior normal distribution $\mathcal{N}(\mu_a, \sigma_{a,ESS}^2)$. The variance
 232 $\sigma_{a,ESS}^2$ was fixed such that the information introduced by the prior would be equivalent to the information
 233 introduced by a fixed number of patients, which was calibrated to control the amount of information²⁴.
 234 This approach is based on the effective sample size (ESS): the higher the ESS, the more informative
 235 the prior. The variable m was set to a fixed hypothetical number of patients and $\mathbf{Y}_m = (Y_1, \dots, Y_m)$ is the
 236 associated pseudo-data vector. The likelihood of \mathbf{Y}_m is $f_m(\mathbf{Y}_m|a) = \prod_{i=1}^m f(Y_i; a)$, where $f(Y_i; a)$ is the
 237 marginal likelihood obtained after integrating the likelihood of Eq. 1 with respect to the efficacy and the
 238 dose. Then, a non-informative prior $q_0(a)$ is introduced with the same expectation μ_a and a very large
 239 variance. The ESS is defined as the sample size m such that the posterior $q_m(a) \propto q_0(a) \times f_m(\mathbf{Y}_m|a)$ is
 240 very close to $\pi_{ESS}(a)$. The proximity between q_m and $\pi_{ESS}(a)$ is evaluated by the distance between
 241 the second derivatives of $\pi_{ESS}(a)$ and q_m with respect to a , $I_\pi(a, \mu_a, \sigma_{a,ESS}^2) = \frac{\partial^2}{\partial a^2} \log \pi_{ESS}(a)$ and
 242 $I_{q_m}(a, m, \mu_a, \sigma_{a,ESS}^2) = \int \frac{\partial^2}{\partial a^2} \log q_m(a) d f_m(\mathbf{Y}_m|a)$:

$$\delta(m, \mu_a, \sigma_{a,ESS}^2) = |I_\pi(\bar{a}, \mu_a, \sigma_{a,ESS}^2) - I_{q_m}(\bar{a}, m, \mu_a, \sigma_{a,ESS}^2)| \quad (9)$$

243 where \bar{a} is the empirical mean of a , which is fixed using the pooling method³² previously introduced
 244 in the specification of the WMs. For an ESS m^* , parameters $(\mu_a, \sigma_{a,ESS}^2)$ were chosen such that
 245 $\min_m \delta(m, \mu_a, \sigma_{a,ESS}^2) = m^*$. Details of the δ expression can be found in Appendix B.

247 **Option Least informative prior (AP_{LIP}-bCRM).** Another method proposed by Zhang *et al.*²⁷ considers
 248 only information from the dose-toxicity model. Let $\pi_{LIP}(a)$ follow $\mathcal{N}(\mu_a, \sigma_{a,LIP}^2)$. The variance $\sigma_{a,LIP}^2$
 249 was defined such that all doses had the same probability of being the MTD. The parameter space of a
 250 was divided into K intervals $\mathcal{I}_1 = [a_0, a_1], \mathcal{I}_2 = [a_1, a_2], \dots, \mathcal{I}_i = [a_{i-1}, a_i], \dots, \mathcal{I}_K = [a_{K-1}, a_K]$, where
 251 a_0 and a_K were the minimal and maximal possible values of a (resp. defined with $\psi(d_1, a_0) = \tau + 0.05$
 252 and $\psi(d_K, a_K) = \tau - 0.05$) and a_1, \dots, a_{K-1} were the solutions of $\psi(d_i, a_i) + \psi(d_{i+1}, a_i) = 2\tau$ (value such
 253 that dose i was the MTD). The method theoretically verifies that parameter a had the same chances of
 254 belonging to the K intervals $\mathcal{I}_1, \mathcal{I}_2, \dots, \mathcal{I}_K$. Therefore, σ_a^2 is calculated such that the empirical variance of
 255 the K probabilities of toxicity matches the variance of a discrete uniform distribution $(K^2 - 1)/12$ ²⁷.

257 However, the resulting variances $\sigma_{a,ESS}^2$ and $\sigma_{a,LIP}^2$ may be too narrow, leading to difficulties in reaching
 258 the extremes in the dose-range (minimum and/or maximum doses). Both options were combined with
 259 the adaptive prior method, which was introduced by Zhang *et al.*^{26;27} and was used when the probability
 260 of the MTD being the smallest or the highest dose was high. A second prior $\pi_{NIP}(a) \sim \mathcal{N}(\mu_a, \sigma_{a,NIP}^2)$,
 261 which is considered a non-informative prior, was associated with a higher variance $\sigma_{a,NIP}^2$ defined from
 262 the former intervals $\mathcal{I}_1, \mathcal{I}_2, \dots, \mathcal{I}_K$ such that $\sigma_{a,NIP}^2$ verified $\Pr(a \in \mathcal{I}_1 \cup \mathcal{I}_K) = 0.80$.

264 The decision to switch from $\pi_{ESS}(a)$ to $\pi_{NIP}(a)$ (option ESS; AP_{ESS}-bCRM) or from $\pi_{LIP}(a)$ to
 265 $\pi_{NIP}(a)$ (option least informative prior; AP_{LIP}-bCRM) was performed using the Bayes factor model
 266 selection criterion. Three models were defined, each with a uniform distribution: $M_1 : a \in \mathcal{I}_1$; $M_2 : a \in$
 267 $\mathcal{I}_2 \cup \dots \cup \mathcal{I}_{K-1}$ and $M_3 : a \in \mathcal{I}_K$ with a uniform distribution within each model. This gave:

$$\Pr(\mathbf{Y}_m|M_1) = \int_{a_0}^{a_1} \prod_{i=1}^K \psi(d_i, a)^{y_i} (1 - \psi(d_i, a))^{1-y_i} \frac{1}{a_1 - a_0} da$$

268 for model M_1 and similar equations can be derived for $\Pr(\mathbf{Y}_m|M_2)$ and $\Pr(\mathbf{Y}_m|M_3)$. The Bayes factor were
269 calculated as follows:

$$\Pr(M_1|\mathbf{Y}_m) = \frac{\Pr(M_1)\Pr(\mathbf{Y}_m|M_1)}{\Pr(M_1)\Pr(\mathbf{Y}_m|M_1) + \Pr(M_2)\Pr(\mathbf{Y}_m|M_2) + \Pr(M_3)\Pr(\mathbf{Y}_m|M_3)}$$

270 where $\Pr(M_1) = \Pr(M_2) = \Pr(M_3) = 1/3$, and similar equations can be obtained for $\Pr(M_2|\mathbf{Y}_m)$ and
271 $\Pr(M_3|\mathbf{Y}_m)$. Using the rule proposed by Zhang *et al.*²⁷, the following criteria was used: If $\Pr(M_3|\mathbf{Y}_m) >$
272 0.61 (Jeffrey's rule), there was substantial evidence that model M_3 was more likely to be true, and a change
273 from prior $\pi_{ESS}(a)$ or $\pi_{LIP}(a)$ to $\pi_{NIP}(a)$ was thus made.

274 In practice, a comparison was performed between AP_{ESS}-bCRM which used the bCRM with the adaptive
275 prior from $\pi_{ESS}(a)$ to $\pi_{NIP}(a)$, and the AP_{LIP}-bCRM which used the bCRM adaptive prior from $\pi_{LIP}(a)$
276 to $\pi_{NIP}(a)$, respectively.

277 3 Simulations

278 The aim of the simulation study was to evaluate and compare the performances of each dose-range and
279 model setting proposition, in terms of selected dose. Based on the motivating illustration, we proposed to
280 plan, conduct and analyse a hypothetical phase I/II dose-finding clinical trial for erlotinib in the paediatric
281 population. We used PK parameters as well as dose-finding toxicity and efficacy clinical trial data for
282 erlotinib obtained from the adult population for extrapolation and bridging.

283 **(1) Specification of the dose-range:** We hypothesised that the observed AUC in adults was similar in
284 the paediatric population for the three dose-range adjustments LA, AA and MA (linear, allometric and

285 maturation adjustments). In previous adult dose-finding studies, the doses ranged from 100 mg to 300 mg
 286 and the MTD was 150 mg^{7;8}. Based on these publications, the adult doses 100 mg, 150 mg, 200 mg,
 287 250 mg and 300 mg were chosen as references for the calculation of paediatric doses. The corresponding
 288 doses for children were extrapolated using the adult PK data published by Lu *et al.*³³, which describe
 289 the erlotinib PK as a one-compartment model with a clearance of 3.95 L/h. The maturation functions for
 290 erlotinib used in the MA [option](#) can be found in Appendix C. The dose-ranges associated with each [option](#)
 291 (LA, AA and MA) for patients aged 2 to 5 years were generated according to Eqs. 2, 3 and 6, respectively.
 292 The resulting dose-range for each [option](#), which were rounded up to the nearest 5 mg/kg, are given in
 293 Table 1.

294 **(2) Choice of WMs using adult information:** A WM needed to be specified for the initial dose-toxicity
 295 relationships associated with each dose-range adjustment. These WMs were elaborated as described in
 296 the Methods section with a mixture of PK, toxicity and efficacy data from adults. In the erlotinib setting,
 297 the mixture was constructed using toxicity data and PK data from early-phase clinical trials in adults
 298 (Figure 2). First, the toxicities associated with doses for children $\gamma_\ell^{(1)}$, $\ell = 1, \dots, 4$ were extrapolated using
 299 PK data published by Thomas *et al.* under the assumption that the same exposure was achieved in the
 300 adult and paediatric populations (AUC relationship with dose and clearance; Table 2)³⁴. Second, using
 301 the pooled data analysis proposed by Zohar *et al.* and based on adult toxicity data from seven clinical
 302 trial studies on erlotinib, the second estimate $\gamma_\ell^{(2)}$ was computed³² for each dose ℓ (computation details
 303 are given in the Appendix A). These clinical studies have reported that different dose levels of erlotinib
 304 induce toxicity, defined as skin rash of grade 3 or more in adults. This information and the estimates of
 305 $\gamma_\ell^{(2)}$, $\ell = 1, \dots, 4$ are summarized in Table 2. The resulting estimated mixture $\gamma_\ell^{(T)}$ associated with each dose
 306 ℓ can also be found in Table 2. Because the dose-range obtained with the different approaches (LA, AA or
 307 MA) overlap and might correspond to different doses within the adult range, a logistic function was fit to
 308 the mixture. The resulting logit function is given by $\eta(d) = \text{logit}^{-1} \left(-3.78 + 0.06 \frac{d}{Cl_{ch}} \right)$, where Cl_{ch} is
 309 the average clearance across in 2 to 5 year old children. Given the dose-ranges generated as described
 310 in the previous section and $\eta(d)$, the first working model (WM1), computed with Eq. 7 was obtained by

311 reading the toxicities associated with each dose from the curve (Table 1). Then, WM2 and WM3 were
 312 computed using Eq. 8.

313 For efficacy, data from adults treated for glioblastoma were considered because efficacy is strongly related
 314 to the specific disease. In this setting, efficacy was defined as remission or stability regarding tumour
 315 size according to RECIST criteria. Because most of the data were associated with one dose, a method
 316 developed by Chung *et al.* was used to obtain the WM. The percentage of efficacy over all available
 317 published data (Table 2) was 20%. We obtained the WM for efficacy reported in Table 1 using the function
 318 `getprior(halfwidth = 0.05, target = 0.2, nu = 2, nlevels = 5)` available in the `dferm` package in R³⁵.

319 **(3) Specification of prior densities:** The prior densities for dose toxicity and dose efficacy parameters
 320 $\pi_{ESS}(a)$, $\pi_{LIP}(a)$, $\pi_{NIP}(a)$ and $\pi(b)$ are given in Table 1.

321 With the ESS option, μ_a and $\sigma_{a,ESS}^2$, the pooling method employed for the WM specification³² with a
 322 power model, resulting in an estimate of the empirical mean $\bar{a} = \log(0.88)$; thus, $E[\exp(a)] = e^{\mu_a + \sigma_{a,ESS}^2/2}$.

323 The expected chosen sample size was $m^* = 5$ patients and $\sigma_{a,ESS}^2$ was then computed with Eq. 9.

324 Then, $\sigma_{a,LIP}^2$ was calculated with the least informative prior option, and $\sigma_{a,NIP}^2$ was calculated using $K = 5$
 325 intervals by minimising $\Pr(a \in \mathcal{I}_1 \cup \mathcal{I}_K) - 0.80 = 0$.

326 For efficacy, prior $\pi(b)$ was selected as a non-informative normal distribution $\mathcal{N}(0, 1.34)$.

327 The performances of our unified approach were investigated through a simulation study under several
 328 scenarios presented in Figure 3 for the three dose-ranges options (LA, AA, and MA). Extrapolation from
 329 adults yielded an initial estimate of 48 mg/kg for the MTD associated with a toxicity target of 0.25. We
 330 aimed to evaluate how this choice influences the performance of our proposed methods by selecting
 331 scenarios in which the MTD and sMSD were different. Scenarios 1, 2 and 3 were based on the results
 332 of two real paediatric trials conducted by Georger *et al.*¹⁴ and Jakacki *et al.*¹⁵. For all three scenarios,
 333 we considered the same MTD that was found in each trial and the efficacy was simulated. In scenarios
 334 1 and 2, the MTD (83 mg/kg) is equal to that reported by Georger *et al.* and is far from the efficacy
 335 extrapolated from adult information (48 mg/kg). In scenario 1, the sMSD was similar to the MTD, whereas
 336 in scenario 2, the sMSD was 65 mg/kg. In scenario 3, the MTD and the sMSD are equals to those reported

337 by Jakacki *et al.* (55 mg/kg) and close to the value extrapolated from adult information. Finally, we added
338 three scenarios: in scenario 4, the MTD (65 mg/kg) was equivalent to the MSD; in scenario 5, the MSD
339 was higher than the MTD (45 mg/kg); and in scenario 6, the sMSD is similar to the MTD (70 mg/kg).
340 For each scenario, we performed 1,000 simulated phase I/II trials with a maximal sample size of $N = 50$
341 patients. Because maturation is known to differ among different paediatric age subgroups, we selected a
342 paediatric population with an age range of 2 to 5 years. We also chose a toxicity target of $\tau = 0.25$ and a
343 minimum efficacy target of $\tau' = 0.20$ (a realistic target for glioblastoma).
344 For each approach, the percentage of correct dose selection (PCS) of the sMSD was computed. We
345 also evaluated the percentage of acceptable doses (ADs) that includes the closest dose to the sMSD
346 for each approach; if this dose existed, we evaluated the next lower dose for which the probability of
347 success P was included in $[P(\text{sMSD}) - 0.05; P(\text{sMSD})]$. For the three dose-range options (LA, AA
348 and MA), we evaluated the methods as follows: (i) option unique WM (WM1-bCRM) compared with
349 WAIC (WAIC-bCRM) using a non-informative prior ($\mathcal{N}(0, 1.34)$) for parameter a of the dose-toxicity
350 relationship, and (ii) adaptive prior under option ESS (AP_{ESS}-bCRM) compared with adaptive prior under
351 option Least informative prior (AP_{LIP}-bCRM).

352 [Table 1 about here.]

353 [Figure 2 about here.]

354 [Figure 3 about here.]

355 [Table 2 about here.]

356 4 Results

357 Based on the toxicity results reported by Geoerger *et al.*¹⁴, scenarios 1 and 2 shared the same MTD of
358 83 mg/kg. However, the sMSDs differed depending on the efficacy differed with 83 mg/kg for scenario 1
359 and 65 mg/kg for scenario 2 (Figure 3).

360 The LA, for a dose of 83 mg/kg dose was out of range; thus, for scenario 1, the last dose (70 mg/kg) was
361 the only option for the recommended dose. The obtained PCSs for all options was greater than 70%, and
362 in approximately 10% of cases, the trials was stopped due to inefficiency (Table 3). In scenario 2, the exact
363 dose of 65 mg/kg dose was not within the dose-range, and the closest dose was 70 mg/kg. As a result,
364 the model hesitated between doses of 55 mg/kg and 70 mg/kg. In this case, the adaptive prior and WAIC
365 options recommended doses between these two values for approximately half of the trials. Using the AA
366 option, the closest corresponding dose to the sMSD was 80 mg/kg in scenario 1, and the PCS ranged from
367 45.2% to 59.1% for all methods. However, because the probability of success for the doses 65 mg/kg and
368 80 mg/kg doses in scenario 1 (the green area under the curve of $P(d)$) were very close, both doses were
369 considered admissible. In this case, the percentage of AD was greater than 94%. In scenario 2, the sMSD
370 was 65 mg/kg, and the PCS was greater than 90% for all options. With the MA, the sMSD was not within
371 the dose-range; thus, the model hesitated between two doses with average percentages of AD equal to
372 90% for scenario 1 and 50% for scenario 2.

373 In scenario 3, the sMSD was equal to the MTD (i.e., the 54 mg/kg dose). In the case of AA, the closest
374 dose to the MTD was 50 mg/kg, and the PCSs for all options were greater than 71%.

375 In scenario 4, the sMSD and MTD were similar (the 65 mg/kg dose). In the case of AA, the dose was within
376 the dose-range, and the PCSs of WAIC-bCRM and WM1-bCRM were 70.5% and 75.2%, respectively.
377 However, the AP_{ESS}-bCRM gave a lower PCS (63.9%) compared with that obtained with the AP_{LIP}-bCRM
378 (73.6%). In scenario 5, the recommended dose was 45 mg/kg, which is within the dose-range obtained
379 with LA and MA. In this case, all options gave high PCS values greater than 60%. If the dose was not
380 within the range, as was the case with AA, the PCS decreased an average of 10%. In scenario 6, the
381 recommended dose was 70 mg/kg. Even if the dose was only in the ranges obtained with the LA and MA
382 options, high PCS values (above 90%) were obtained for all dose-range options.

383 The comparison of the performances of AP_{ESS}-CRM and AP_{LIP}-CRM, revealed similar performances
384 over all dose-range options and scenarios. However, WM1-bCRM and WAIC-bCRM generally provided
385 better recommendations in terms of the admissible dose.

386 In the case of a too-toxic scenario (sMSD of 20 mg/kg, data not shown), the stopping rules allowed the
387 trial to be stopped if a toxic reaction was observed in 90% of the cases, regardless of the method.

388 In general, if the sMSD was within the dose-range, the PCS and AD percentages were high, whereas if the
389 dose was close but not within the range, a lower PCS percentage and a rather high AD percentage were
390 obtained.

391 [Table 3 about here.]

392 5 Guidelines

393 Based on the results of our simulations, we suggest the following settings for the proposed approach:

- 394 1. For dose-range selection: use either options AA or MA.
- 395 2. For the WM choice: use option WAIC-bCRM because our results indicates that it is better to use
396 several WMs in the model selection process than a unique WM.
- 397 3. For prior distribution: if the quantity and quality of the adult information is high, use the AP_{ESS} -
398 bCRM option; however, if there is some doubt regarding the available adult information, use the
399 AP_{LJP} -bCRM option.

400 6 Discussion

401 In this work, we present a unified approach for planning, conducting and analysing paediatric dose-finding
402 clinical trials. This unified approach is based on several possible methods that aim to improve the choices
403 made in the design of paediatric trials. For the analysis of the paediatric population, for which only a small
404 number of clinical trials have been conducted and which typically includes a small number of patients, the
405 bridging of information from the adult population (when possible) to the paediatric population, particularly
406 using PK extrapolation tools such as allometry and maturation functions, is highly relevant.

407 We based our unified method on the bCRM, which jointly models toxicity and efficacy with a dose-finding
408 allocation rule because in paediatric populations, safety takes priority over efficacy. Our unified approach
409 includes all stages in the dose-finding process, ranging from dose-range selection to the choice of prior
410 distributions for dose responses.

411 The first step of our work proposed three different dose-range adjustments (i.e., linear, allometry or
412 maturation adjustment (LA, AA or MA)). The resulting dose-ranges overlapped, and a wider range was
413 obtained with AA. In this study, we used the specific context of erlotinib, a drug that has been investigated
414 in both adult and paediatric populations for cancer treatment. Both dose-finding and PK studies in adults
415 and children are available. We thus used the available adult information to plan a paediatric trial using the
416 proposed extrapolation and bridging methods and used the children's dose-finding data to build scenarios
417 for the simulation study, which allowed us to evaluate our design choices.

418 Our extrapolation and bridging approach used data from more than 580 adult observations. We based three
419 of our scenarios for the simulation study on the toxicity observations reported by Georger *et al.*¹⁴ and
420 Jakacki *et al.*¹⁵, who performed trials that evaluated 16 and 19 children, respectively. Thus, the estimation
421 of the MTD or recommended dose in each trial was associated with high variability due to the small
422 sample size. In this case, it is difficult to assess how far from reality is our model from the true paediatric
423 population. In general, our results show that in cases in which the MTD and sMSD are far from our initial
424 guess (as in scenarios 1 and 2), our proposed dose-finding designs based on either model selection criteria
425 or adaptive priors performed well. A similar finding was obtained for scenario 3, in which the MTD and
426 the sMSD were not far from our initial guess. These results are in favour of the implemented methods
427 because misspecified initial choices do not impact the performance of our proposition.

428 To date, there is no clear recommendation for the selection of the dose-range that should be used in
429 paediatric dose-finding clinical trials. Allometric scaling was initially introduced by West *et al.*³⁶ for
430 identifying measurements that work across and within species. Several studies have suggested that the
431 allometric coefficient may be different in early childhood^{36;37}. The discrepancy between size-based scaling

432 and effective changes in paediatric patients, particularly neonates and infants, can also be explained by
433 differences in physiological processes due to maturation.

434 The second step of our work was to propose dose-finding design choices for the dose allocation process
435 using adult clinical trial observations. Because not all of the calculated doses were used for adults, we
436 needed to build a logit function based on mixture estimates in adults. For this purpose, we assumed that
437 the exposure was similar in both adults and children. Adult pharmacokinetics combined with maturation
438 served as the first source of information for the toxicity probability, which was defined in terms of PK
439 (AUC or C_{max}). A direct curve was reported by Thomas *et al.*³⁴. The second source of information
440 was toxicity from early-phase clinical trials in adults. This method allowed us to propose tools for the
441 establishment of the WMs and for the prior distributions of dose-toxicity parameters.

442 For simplicity reasons, we maintained the same scenarios for all dose-ranges, which led to different
443 sMSDs. In cases in which the model hesitated between two doses, a lower PCS was obtained primarily
444 because the real dose was not exactly within the dose-range. Other scenario choices could have favoured
445 one adjustment method over the other, although this situation occurred due to arbitrary choices. Other
446 methods that jointly model toxicity and efficacy for dose-finding, such as EFFTOX, can also benefit from
447 our proposed approach, although some may only need to use part of our model¹⁶. In our case, power
448 function modelling of the dose-toxicity or dose-efficacy curves was selected for simplicity. However,
449 several other models, such as the logit model, could easily be used in our setting.

450 In conclusion, the bridging and extrapolation of adult data for the design of paediatric dose-finding clinical
451 trials appear to improve the results of these studies. Our proposition may prove helpful for physicians
452 and statisticians who wish to plan and conduct early-phase trials in this population. We attempted to unify
453 and modify existing methods to obtain a clear stream of decision-making regarding several crucial choices
454 that need to be made prior to initiation of a trial. We believe that this approach will improve and allow
455 better use of the available information sources for the planning of new trials.

Aknowledgements

Caroline Petit was supported during this work by a grant IDEX from the Université Sorbonne Paris Cité (2013, project 24). Sarah Zohar, Emmanuelle Comets and Moreno Ursino were funded by the InSPiRe (Innovative Methodology for Small Populations Research) Project of the European Union Seventh Framework Programme for Research, Technological Development, and Demonstration under grant agreement FP HEALTH 2013-602144. During this work, Adeline Samson was partially supported by the LabEx PERSYVAL-Lab (ANR-11-LABX-0025-01) funded by the French program Investissement d'avenir.

References

1. Brasseur D. Paediatric research and the regulation "better medicines for the children in europe". *Eur J Clin Pharmacol*, 67 Supp:1–3, 2011.
2. Denne S. Pediatric clinical trial registration and trial results: An urgent need for improvement. *Pediatrics*, 129:1320–1, 2012.
3. Thall P.F., Nguyen H.W., Zohar S., and Maton P. Optimizing sedative dose in preterm infants undergoing treatment for respiratory distress syndrome. *J Am Stat Assoc*, 109:931–943, 2014.
4. Anderson B.J. and Holford N.H.G. Mechanistic basis of using body size and maturation to predict clearance in humans. *Drug. Metab. Pharmacokinet.*, 24:25–36, 2009.
5. Johnson T.N. The problems in scaling adult drug doses to children. *Arch. Dis. Child.*, 93:207–211, 2008.
6. Dousseau A., Geoerger B., Jiménez I., and Paoletti X. Innovations for phase I dose-finding designs in pediatric oncology clinical trials. *Contemp. Clin. Trials*, 47:217–227, 2016.
7. Prados M.D., Lamborn K.R., Chang S., Burton E., Butowski N., Malec M., Kapadia A., Rabbitt J., Page M.S., Fedoroff A., Xie D., and Kelley S.K. Phase 1 study of erlotinib HCl alone and combined with temozolomide in patients with stable or recurrent malignant glioma. *Neuro. Oncol.*, 8:67–78, 2006.
8. Thepot S., Boehrer S., Seegers V., Prebet T., Beyne-Rauzy O., Wattel E., Delaunay J., Raffoux E., Hunault M., Jourdan E., Chermat F., Sebert M., Kroemer G., Fenaux P., Adès L., and Groupe Francophone des

- 481 Myelodysplasias (GFM). A phase I/II trial of erlotinib in higher risk myelodysplastic syndromes and acute
482 myeloid leukemia after azacitidine failure. *Leuk Res.*, 38:1430–4, 2014.
- 483 9. Calvo E., Malik S.N., Siu L.L., Baillargeon G.M, Irish J., Chin S.F., Santabarbara P., Kreisberg J.I., Rowinsky
484 E.K., and Hidalgo M. Assessment of erlotinib pharmacodynamics in tumors and skin of patients with head and
485 neck cancer. *Ann. Oncol.*, 18:761–7, 2007.
- 486 10. Raizer J., Abrey L., Lassman L., Chang S., Lamborn K., Kuhn J., Yung A., Gilbert M., Aldape K., Wen P., Fine
487 H., Mehta M., DeAngelis L., Lieberman F., Cloughesy T., Robins H., Dancey J., and Prados P. for the North
488 American Brain Tumor Consortium. A phase II trial of erlotinib in patients with recurrent malignant gliomas and
489 nonprogressive glioblastoma multiforme postradiation therapy. *Neuro-Oncology*, 12:95–103, 2010.
- 490 11. van den Bent M., Brandes A., Rampling R., Kouwenhoven M., Kros J., Carpentier A., Clement P., Frenay M.,
491 Campone M., Baurain J-F., Armand J-P., Taphoorn M., Tosoni A., Kletzl H., Klughammer B., Lacombe D., and
492 Gorlia T. Randomized phase II trial of erlotinib versus temozolomide or carmustine in recurrent glioblastoma:
493 Eortc brain tumor group study 26034. *J. Clin. Oncol.*, 27:1258–74, 2009.
- 494 12. Sheikh N. and Chambers C. Efficacy vs. effectiveness: Erlotinib in previously treated non-small-cell lung cancer.
495 *J Oncol Pharm Practice*, 19:228–236, 2012.
- 496 13. Hoffmann-La Roche. A study of management of tarceva - induced rash in patients with non-small
497 cell lung cancer. Available at [https://clinicaltrials.gov/ct2/show/NCT00531934?term=](https://clinicaltrials.gov/ct2/show/NCT00531934?term=00531934&rank=1)
498 [00531934&rank=1](https://clinicaltrials.gov/ct2/show/NCT00531934?term=00531934&rank=1), February 2015. NCT00531934.
- 499 14. Georger B., Hargrave D., Thomas F., Ndiaye A., Frappaz D., Andreiuolo F., Varlet P., Aerts I., Riccardi R.,
500 Jaspan T., Chatelut E., Le Deley M.C., Paoletti X., Saint-Rose C., Leblond P., Morland B., Gentet J.C., Méresse
501 V., Vassal G., and ITCC (Innovative Therapies for Children with Cancer) European Consortium. Innovative
502 therapies for children with cancer pediatric phase I study of erlotinib in brainstem glioma and relapsing/refractory
503 brain tumors. *Leuk Res.*, 38:1430–4, 2011.
- 504 15. Jakacki R., Hamilton M., Gilbertson R., Blaney S., Tersak J., Krailo M., Ingle A., Voss S., Dancey J., and
505 Adamson P. Pediatric phase I and pharmacokinetic study of erlotinib followed by the combination of erlotinib
506 and temozolomide: A children’s oncology group phase I consortium study. *J. Clin. Oncol.*, 26:4921–27, 2008.

-
- 507 16. Thall P. and Cook J. Dose-finding based on efficacy-toxicity trade-offs. *Biometrics*, 60:684–693, 2004.
- 508 17. Zohar S. and O’Quigley J. Identifying the most successful dose (msd) in dose-finding studies in cancer.
509 *Pharmaceut. Statist.*, 5:187–199, 2006.
- 510 18. Pressler R., Boylan G., Marlow N., Blennow M., Chiron C., Cross J., de Vries L., Hallberg B., Hellström-
511 Westas L., Jullien V., Livingstone V., Mangum B., Murphy B., Murray D., Pons G., Rennie J., Swarte R., Toet
512 M., Vanhatalo S., Zohar S., and NEonatal seizure treatment with Medication Off-patent (NEMO) consortium.
513 Bumetanide for the treatment of seizures in newborn babies with hypoxic ischaemic encephalopathy (nemo): an
514 open-label, dose finding, and feasibility phase 1/2 trial. *Lancet Neurol*, 14:469–77, 2015.
- 515 19. Broglio K., Sandalic L., Albertson T., and Berry S. Bayesian dose escalation in oncology with sharing of
516 information between patient population. *Contemp. Clin. Trials*, 44:56–63, 2015.
- 517 20. Liu S., Pan H., Xia J., Huang Q., and Yuan Y. Bridging continual reassessment method for phase I clinical trials
518 in different ethnic populations. *Stat. Med.*, 34:1681–1694, 2015.
- 519 21. Yin G. and Yuan Y. Bayesian model averaging continual reassessment method in phase I clinical trials. *JASA*,
520 104:954–968, 2009.
- 521 22. Daimon T., Zohar S., and O’Quigley J. Posterior maximization and averaging for Bayesian working model choice
522 in the continual reassessment method. *Stat. Med.*, 30:1563–73, 2011.
- 523 23. Watanabe S. *Asymptotic Equivalence of Bayes cross validation and widely applicable information criterion in*
524 *singular learning theory*, volume 11. 2010.
- 525 24. Morita S., Thall P.F., and Müller P. Determining the effective sample size of a parametric prior. *Biometrics*,
526 64:595–602, June 2008.
- 527 25. Morita S. Application of the continual reassessment method to a phase I dose-finding trial in japanese patients:
528 East meets west. *Stat. Med.*, 30:2090–2097, July 2011.
- 529 26. Lee S. and Cheung Y. Calibration of prior variance in the bayesian continual reassessment method. *Stat. Med.*,
530 30:2081–89, 2011.
- 531 27. Zhang J., Braun T., and J. Taylor. Adaptive prior variance calibration in the bayesian continual reassessment
532 method. *Stat. Med.*, 32:2221–34, 2013.

-
- 533 28. O'Quigley J., Hughes M., and Fenton T. Dose-finding designs for hiv studies. *Biometrics*, 57:1018–29, 2001.
- 534 29. Petit C., Jullien V., Samson A., Guedj J., Kiechel J.R., Zohar S., and Comets E. Designing a paediatric study for
535 an antimalarial drug including prior information from adults. *Antimicrob. Agents Chemother.*, 60(3):1481–1491,
536 2015.
- 537 30. Price P., Conolly R., Chaisson C., Gross E., Young J., Mathis E., and Tedder D. Modeling inter-individual
538 variation in physiological factors used in pbpk models of humans. *Crit. Rev. Toxicol.*, 33:469–503, 2003.
- 539 31. The Lifetime Group. P³M. *Software available at [http://www.thelifelinegroup.org/p3m/](http://www.thelifelinegroup.org/p3m/library.php)*
540 *library.php*. Version 1.3.
- 541 32. Zohar S., Katsahian S., and O'Quigley J. An approach to meta-analysis of dose-finding studies. *Stat. Med.*,
542 30:2109–2116, 2011.
- 543 33. Lu J-F., Eppler S. M., Wolf J., Hamilton M., Rakhit A., Bruno R., and Lum B. L. Clinical pharmacokinetics
544 of erlotinib in patients with solid tumors and exposure-safety relationship in patients with non-small cell lung
545 cancer. *Clin Pharmacol Ther*, 80:136–45, 2006.
- 546 34. Thomas F., Rochaix P., White-Koning M., Hennebelle I., Sarini J., Benlyazid A., Malard L., Lefebvre J.L.,
547 Chatelut E., and Delord J.P. Population pharmacokinetics of erlotinib and its pharmacokinetic/pharmacodynamic
548 relationships in head and neck squamous cell carcinoma. *Eur J Cancer*, 45:2316–23, 2009.
- 549 35. Ken Cheung. Package 'dfcrm'. *Available at [https://cran.r-project.org/web/packages/](https://cran.r-project.org/web/packages/dfcrm/dfcrm.pdf)*
550 *dfcrm/dfcrm.pdf*, August 2013. Version 0.2-2.
- 551 36. West G.B., Brown J.H., and Enquist B.J. A general model for the origin of allometric scaling laws in biology.
552 *Science*, 276:122–126, April 1997.
- 553 37. Peeters M.Y.M., Allegaert K., Blussé van Oud-Albas H.J., Cella M., Tibboel D., Danhof M., and Knibbe C.A.J.
554 Prediction of propofol clearance in children from an allometric model developed in rats, children and adults
555 versus a 0.75 fixed-exponent allometric model. *Clin. Pharmacokinet.*, 49:269–275, 2010.
- 556 38. Anderson B.J. and Holford N.H.G. Mechanism-based concepts of size and maturity in pharmacokinetics. *Annu.*
557 *Rev. Pharmacol. Toxicol.*, 48:303–332, 2008.

-
- 558 39. Rakhit A., Pantze M., Fettner S., Jones H., Charoin J-E., Riek M., Lum B., and Hamilton M. The effects
559 of CYP3A4 inhibition on erlotinib pharmacokinetics: computer-based simulation (SimCYP) predicts in vivo
560 metabolic inhibition. *Eur. J. Clin. Pharmacol.*, 64:31–41, 2008.
- 561 40. Johnson T.N., Rostami-Hodjegan A., and Tucker G.T. Prediction of the clearance of eleven drugs and associated
562 variability in neonates, infants and children. *Clin. Pharmacokinet.*, 45:931–956, 2006.

A Appendix - Pooling method

The retrospective pooled data method evaluates retrospectively data from several clinical trials. It aims at estimating the parameter of a toxicity model from several models. Let $n_i(j) = \sum_{l=1}^j \mathbb{1}(x_l = d_i)$ be the number of observations at dose level d_i after j patients and $t_i(j) = \sum_{l=1}^j y_l \mathbb{1}(x_l = d_i)$ the number of toxicities observed at dose level d_i among the first j patients. The following approach allows to compute an estimate of the parameter a :

1. First, gather the number of observed DLTs at each dose level t_i ($i = 1, \dots, k$) and the number of patients included at each dose level, n_i , from all available clinical trials.
2. Then, compute the empirical probability of toxicity associated with each dose level by dividing t_i by n_i .
3. For each dose i , after n patients, define a weight $w_n(d_i)$. It is calculated by a simulation study based on a model of interest and marginal frequencies provided by observations. To calculate these weights, we simulate CRM studies of size n under the scenario generated by the empirical probability of toxicities. The weights $w_n(d_i)$ are the percentages of the total allocation for each dose level d_i .
4. Estimate \hat{a} , the estimate of parameter a , by solving

$$W_n(a) = \sum_{i=1}^k w_n(d_i) U_{in}(a) = 0$$

and

$$U_{in}(a) = H\{n_i(n)\} \left[\frac{t_i(n)}{n_i(n)} \frac{\Psi'}{\Psi}(d_i, a) + \left\{ 1 - \frac{t_i(n)}{n_i(n)} \right\} \times \frac{-\Psi'}{1 - \Psi}(d_i, a) \right] \quad i = 1, \dots, k$$

where the coefficient $H(s) = \mathbb{1}(s \neq 0)$, i.e., a function taking the value 1 when s is not equal to 0, and zero otherwise, and, in order to cover all cases, we use the convention that $0/0$ is equal to 1. $U_{in}(a)$ can be interpreted as a score representing the weighted average across the dose level. This is the

580 average of some function of the dose toxicity working model for the patients experiencing toxicity
581 and an average of a similar function of the dose toxicity working model for the non-toxicities.

582 5. An estimate for the probability of toxicity at each of the available dose levels i can be computed
583 with $\psi(d_i, \hat{a})$.

584 In the present paper, for the adult doses of $(d_1, d_2, d_3, d_4) = (100 \text{ mg}, 150 \text{ mg}, 200 \text{ mg and } 250 \text{ mg})$ with
585 a power model $\psi(d_i, a) = \alpha_i^a$ we obtained the observed toxicity probabilities t_i/n_i of $(0, 0.37, 0.11, 0.50)$
586 respectively, the weights w_i $(0.02, 0.31, 0.31, 0.36)$, which lead to the resulting estimate of $\hat{a} = 0.88$ and
587 the following estimates of the probability of toxicity $(0.07, 0.19, 0.35, 0.49)$.

588 B Appendix - Prior specification

589 We defined $q_0(a)$ as a normal $\mathcal{N}(\mu_a, c\sigma_a^2)$ where $c = 10,000$. We first calculated I_{q_m} :

$$590 \quad q_m(a) \propto \frac{1}{\sqrt{2\pi c\sigma_a^2}} e^{-\frac{1}{2c\sigma_a^2}(a-\mu_a)^2} \times \prod_{j=1}^m \psi(a, x_j)^{Y_j} (1 - \psi(a, x_j))^{(1-Y_j)}$$

591 For the j^{th} patient receiving dose x_j , let $[x_j] = 1, \dots, K$ the number giving the corresponding dose subscript.

592 We have the derivative and second derivative:

$$593 \quad \begin{aligned} \frac{\partial \log q_m}{\partial a}(a) &= -\frac{(a-\mu_a)}{c\sigma_a^2} + \log(\alpha_{[x_j]}) \sum_{j=1}^m \left(Y_j \exp(a) - (1-Y_j) \frac{\exp(a)\alpha_{[x_j]}^{\exp(a)}}{1-\alpha_{[x_j]}^{\exp(a)}} \right) \\ \frac{\partial^2 \log q_m}{\partial a^2}(a) &= -\frac{1}{c\sigma_a^2} + \log(\alpha_{[x_j]}) \exp(a) \sum_{j=1}^m \left(Y_j - (1-Y_j) \frac{\alpha_{[x_j]}^{\exp(a)} (1 + \exp(a) \log(\alpha_{[x_j]}) - \alpha_{[x_j]}^{\exp(a)})}{(1-\alpha_{[x_j]}^{\exp(a)})^2} \right) \end{aligned}$$

594 Therefore, we had

$$I_{qm}(a, m, \mu_a, \sigma_a^2) = -\frac{1}{c\sigma_a^2} + \int_{Y_m} \int_{X_m} \sum_{j=1}^m \log(\alpha_{[x_j]}) \exp(a) \left(Y_j - (1 - Y_j) \frac{\alpha_{[x_j]}^{\exp(a)} \left(1 + \exp(a) \log(\alpha_{[x_j]}) - \alpha_{[x_j]}^{\exp(a)} \right)}{\left(1 - \alpha_{[x_j]}^{\exp(a)} \right)^2} \right) f(Y_m|X_m) g(X_m) dY_m dX_m$$

where f is the marginal distribution of $Y_m|X_m$ and g the distribution of X_m . We calculated $I_\pi(a) = -\frac{1}{\sigma_a^2}$ and obtained $\delta(m, \mu_a, \sigma_a^2) = |I_\pi(\bar{a}, \mu_a, \sigma_a^2) - I_{qm}(\bar{a}, m, \mu_a, \sigma_a^2)|$.

Since δ was non-computable, due to the dependency of Y_m and X_m , the criterion δ was calculated using Monte-Carlo simulations. In order to calculate (μ_a, σ_a^2) , we computed the *ESS* for several value of (μ_a, σ_a^2) and we chose (μ_a, σ_a^2) such that $\min_m(\delta(m, \mu_a, \sigma_a^2)) = m^*$.

C Appendix - Specification of clearance for erlotinib in children

Erlotinib is administered as tablets. It is partly absorbed by the enterocyte cells. Before reaching the portal vein, a part of erlotinib is metabolised by the cytochrome CYP3A4 through the gut wall and the hepatic barrier. The bioavailability F in adults is 60% with no food intake and 100% otherwise. However, due to ingestion problems, erlotinib is often given with no food intake. We therefore considered a 60% bioavailability. Once in the blood stream, erlotinib bounds to albumin very strongly. The unbound fraction of drug in plasma f_u is 0.05. Erlotinib elimination is mainly hepatic, with a very small renal elimination (about 9%). We neglected that proportion for the maturation process. The cytochrome CYP3A4 is responsible for about 70% of erlotinib elimination while CYP1A2 is responsible for the other 30%³⁹. The adult apparent clearance Cl/F is 3.95 L/h. We assimilated the global clearance to the hepatic clearance Cl_H . Therefore, we can deduce the hepatic extraction ratio with the hepatic plasmatic flow Q_{hep} . The hepatic blood flow is 90 L/h. Correcting by the hematocrit, we obtained $Q = 40.5$ L/h, as reported in Table 4 and we had $E_H = \frac{Cl_H}{Q_{hep}} = \frac{Cl/F \times F}{Q_{hep}} = 0.058$. Considering the hepatic extraction ratio and the fact that CYP1A2, responsible for 30% of the clearance, are not present in the gut wall, we considered a gut wall extraction ration null $E_g = 0$. We then calculated the fraction absorbed $f_{abs} = \frac{F}{1-E_H} = 0.64$. Adult

616 information gathered in Table 4 were used in the computation of paediatric individual clearance. Based on
 617 Eq. 5, we have

$$F_{ch} = f_{abs}(1 - E_G \times MAT_{CYP3A4}(AGE))(1 - E_H \times (0.70 MAT_{CYP3A4}(AGE) + 0.30 MAT_{CYP1A2}(AGE)))$$

618 with the maturation function characterised by T. Johnson⁴⁰ given by $MAT_{CYP3A4}(AGE) = \frac{AGE^{0.83}}{0.31 + AGE^{0.83}}$
 619 and $MAT_{CYP1A2}(AGE) = \frac{AGE^{1.41}}{1.13 + AGE^{1.41}}$. The hepatic clearance Cl_{ch} is related to CYP3A4 and CYP1A2,
 620 which vary with age up to the adults values. As a results, Eq. 4 of the paediatric clearance becomes for
 621 erlotinib:

$$\frac{Cl_{ch}}{F_{ch}} = Cl \times (0.70 MAT_{CYP3A4} + 0.30 MAT_{CYP1A2}) \frac{F}{F_{ch}} \times \left(\frac{W_{ch}}{W_{ad}} \right)^{0.75}$$

622

[Table 4 about here.]

623

		Linear Adjustment - LA					Allometry Adjustment - AA					Maturation Adjustment - MA				
		25	35	45	55	70	35	50	65	80	100	30	45	55	70	85
Doses (mg/kg)																
WMs for toxicity	WM1	0.07	0.13	0.21	0.33	0.55	0.13	0.27	0.48	0.70	0.88	0.10	0.21	0.33	0.55	0.76
	WM2	0.13	0.21	0.33	0.55	0.78	0.27	0.48	0.70	0.88	0.94	0.21	0.33	0.55	0.76	0.88
	WM3	0.04	0.07	0.13	0.21	0.33	0.06	0.13	0.27	0.48	0.70	0.05	0.10	0.21	0.33	0.55
WM for efficacy		0.05	0.20	0.43	0.64	0.79	0.05	0.20	0.43	0.64	0.79	0.05	0.20	0.43	0.64	0.79
Option ESS																
$\pi_{ESS}(a)$		$\mathcal{N}(-0.31, 0.36)$					$\mathcal{N}(-0.38, 0.50)$					$\mathcal{N}(-0.34, 0.42)$				
Option Least Informative Prior																
$\pi_{LIP}(a)$		$\mathcal{N}(-0.31, 0.46)$					$\mathcal{N}(-0.38, 3.13)$					$\mathcal{N}(-0.34, 1.46)$				
$\pi_{NIP}(a)$		$\mathcal{N}(-0.31, 4.33)$					$\mathcal{N}(-0.38, 15.24)$					$\mathcal{N}(-0.34, 8.88)$				
$\pi(b)$		$\mathcal{N}(0, 1.34)$					$\mathcal{N}(0, 1.34)$					$\mathcal{N}(0, 1.34)$				

Table 1. Model settings for simulations. AP_{ESS}-bCMR uses adaptive prior from $\pi_{ESS}(a) \sim \mathcal{N}(\mu_a, \sigma_{a,ESS}^2)$ to $\pi_{NIP}(a) \sim \mathcal{N}(\mu_a, \sigma_{a,NIP}^2)$ and AP_{LIP}-bCRM uses adaptive prior from $\pi_{LIP}(a) \sim \mathcal{N}(\mu_a, \sigma_{a,LIP}^2)$ to $\pi_{NIP}(a)$.

Publications	Response/toxicity (number of patients)			
	100 mg	150 mg	200 mg	250 mg
Toxicity				
Prados <i>et al.</i>	0 (3)	1 (3)	0 (3)	3 (6)
Raizer <i>et al.</i>	-	11 (99)	-	-
Thepot <i>et al.</i>	0 (5)	3 (25)	-	-
Calvo <i>et al.</i>	-	1 (25)	-	-
Van den Bent <i>et al.</i>	-	-	6 (54)	-
Sheikh <i>et al.</i>	-	167 (307)	-	-
Clinical trial ROCHE NTC00531934	-	11 (59)	-	-
$\gamma_{\ell}^{(1)}$	0.13	0.24	0.40	0.59
$\gamma_{\ell}^{(2)}$	0.07	0.19	0.34	0.49
$\gamma_{\ell}^{(T)}$	0.09	0.21	0.36	0.54
Efficacy for glioblastoma at dose 150 mg				
Prados <i>et al.</i>		1 (16)		
Prados <i>et al.</i> (EIAED)		5 (44)		
Raizer <i>et al.</i>		7 (53)		
Yung <i>et al.</i>		20 (48)		

Table 2. Toxicity, efficacy outcomes and the number of treated patients of erlotinib treatment. Toxicities are skin rash of grade 3 or more and efficacy, defined as stable disease and above (RECIST), was limited to glioblastoma. The distributions for calculating the mixture $\gamma_{\ell}^{(T)}$ are given for each dose ℓ with the value of $\gamma_{\ell}^{(1)}$ based on adult PK information and the value of $\gamma_{\ell}^{(2)}$ built with adult toxicities.

Method	Linear Adjustment					Allometry Adjustment					Maturation Adjustment											
	Dose (mg/kg)	25	35	45	55	70	SR	AD	35	50	65	80	100	SR	AD	30	45	55	70	85	SR	AD
Scenario 1																						
WMI-bCRM	0	0	0.3	7.8	<u>81.8</u>	10.1	89.6	0	1.4	<u>39.6</u>	<u>56.8</u>	2.1	0.1	0.1	96.4	0	0.1	8.2	60.4	<u>30</u>	1.3	90.4
WAIC-bCRM	0	0	0.2	8.1	<u>81.7</u>	10	89.8	0	1.2	<u>37.2</u>	<u>59.1</u>	2.3	0.2	0.2	96.3	0	0.3	6.3	53.4	<u>38.3</u>	1.7	91.7
AP _{ESS} -bCRM	0	0	0	14.4	<u>77.9</u>	6.2	92.2	0	1.4	<u>50.9</u>	<u>45.2</u>	2.2	0.2	0.2	96.1	0	0.2	12.2	59.5	<u>26.8</u>	1	86.2
AP _{LIP} -bCRM	0	0	0.1	<u>13.9</u>	<u>77.1</u>	7.1	91	0	1.1	<u>35.1</u>	<u>59.8</u>	3.9	0.1	0.1	94.9	0	0.1	7.3	58.3	<u>32.3</u>	2	90.6
Scenario 2																						
WMI-bCRM	0	0	0.2	51.8	48	0	48	0	6.9	<u>92.7</u>	0.4	0	0	0	92.7	0	0	53	47	0	0	47
WAIC-bCRM	0	0	0.2	44.9	<u>54.8</u>	0.1	54.8	0	7.9	<u>91.7</u>	0.3	0	0.1	0.1	91.7	0	0.1	41.7	<u>58.1</u>	0	0.1	58.1
AP _{ESS} -bCRM	0	0	0	53	<u>47</u>	0	47	0	8	<u>91.8</u>	0.2	0	0	0	91.8	0	0.1	62.6	<u>37.1</u>	0.1	0	37.1
AP _{LIP} -bCRM	0	0	0	51	<u>49</u>	0	49	0	7.8	<u>91.6</u>	0.6	0	0	0	91.6	0	0	52.6	<u>47.4</u>	0	0	47.4
Scenario 3																						
WMI-bCRM	0	0.2	18.7	<u>80.1</u>	0.9	0.1	98.8	1	<u>86.6</u>	12	0	0	0	0.4	86.6	0	<u>18.7</u>	<u>79.6</u>	1.5	0	0.2	98.3
WAIC-bCRM	0	0.2	26.2	72	1.6	0	98.2	1.3	<u>88.1</u>	10.2	0	0	0.4	0.4	88.1	0	<u>25.4</u>	<u>73.5</u>	1.1	0	0	98.9
AP _{ESS} -bCRM	0	0.4	<u>26.1</u>	<u>73</u>	0.5	0	99.1	1.2	<u>89</u>	9.5	0	0	0.2	0.2	89	0.1	<u>27</u>	<u>71.9</u>	1	0	0	98.9
AP _{LIP} -bCRM	0	0.1	<u>24.9</u>	<u>74.2</u>	0.8	0	99.1	0.6	<u>83.6</u>	14.6	0	0	0.9	0.9	83.6	0.4	<u>22</u>	<u>77.1</u>	0.4	0	0.1	99.1
Scenario 4																						
WMI-bCRM	0	0	1.3	<u>61.8</u>	36.9	0	61.8	0.1	23.5	<u>75.2</u>	1.2	0	0	0	75.2	0	1.2	<u>56.3</u>	42.4	0	0.1	56.3
WAIC-bCRM	0	0	4.3	<u>64.7</u>	31	0	64.7	0.2	28.5	<u>70.5</u>	0.7	0	0	0.1	70.5	0	3.4	<u>63.5</u>	33	0	0.1	63.5
AP _{ESS} -bCRM	0	0	3.2	<u>73.4</u>	23.4	0	73.4	0	35.4	<u>63.9</u>	0.4	0	0.3	0.3	63.9	0	2.8	<u>69.8</u>	27.4	0	0.1	69.8
AP _{LIP} -bCRM	0	0	2.5	<u>68.2</u>	29.2	0	68.2	0	25.1	<u>73.6</u>	0.6	0	0.5	0.5	73.6	0	1.1	<u>61.1</u>	37.5	0.1	0.1	61.1
Scenario 5																						
WMI-bCRM	0.9	20.7	<u>61.5</u>	15.9	0	1	61.5	32.5	<u>59.7</u>	0.4	0	0	0	7.4	59.7	10.9	<u>72.2</u>	14.5	0	0	2.4	72.2
WAIC-bCRM	0.1	18.2	<u>68</u>	13	0	0.7	68	36.4	<u>56.7</u>	0.6	0	0	6.3	6.3	56.7	13	<u>70.9</u>	13.7	0	0	2.4	70.9
AP _{ESS} -bCRM	0.7	21.9	<u>65.3</u>	11.7	0	0.4	65.3	40.2	<u>53.8</u>	0.2	0	0	5.8	5.8	53.8	13.4	<u>72.7</u>	12.5	0	0	1.4	72.7
AP _{LIP} -bCRM	0.4	22.5	<u>62.2</u>	14.8	0	0.1	62.2	33.2	<u>57.7</u>	0.4	0	0	8.7	8.7	57.7	11.7	<u>72.1</u>	13.1	0	0	3.1	72.1
Scenario 6																						
WMI-bCRM	0	0	0	2.8	<u>96</u>	1.2	96	0	0	<u>90.4</u>	9.6	0	0	0	90.4	0	0	3.7	<u>96.2</u>	0.1	0	96.2
WAIC-bCRM	0	0	0	6	<u>93.2</u>	0.8	93.2	0	0	<u>94.6</u>	5.4	0	0	0	94.6	0	0	5.5	<u>93.7</u>	0.8	0	93.7
AP _{ESS} -bCRM	0	0	0	7.9	<u>90.1</u>	2	90.1	0	0.1	<u>92.4</u>	7.5	0	0	0	92.4	0	0	5.7	<u>94.3</u>	0	0	94.3
AP _{LIP} -bCRM	0	0	0	5.6	<u>93.4</u>	1	93.4	0	0	<u>87.8</u>	12.2	0	0	0	87.8	0	0	4	<u>95.6</u>	0.4	0	95.6

Table 3. Simulation study results for the three dose-range methods, linear, allometry and maturation adjustment (LA, AA, MA) under several scenarios. The percentage of correct selection (PCS) are represented in italic; that is the sMSD. The percentage of acceptable dose (underlined) are summed up in bold. The simulation setting for each approach are given in Table 1.

Parameters	Value	Source
k_a (h ⁻¹)	0.949	Lu <i>et al.</i> , 2006
Cl/F (L.h ⁻¹)	3.95	Lu <i>et al.</i> , 2006
V/F (L)	233	Lu <i>et al.</i> , 2006
Q (L.h ⁻¹)	40.5	-
Cl_u (L.h ⁻¹)	47.4	-
f_{abs}	0.64	-
f_u	0.05	-
E_G	0	-
E_H	0.058	-

Table 4. Pharmacokinetic parameters used for paediatric extrapolation.

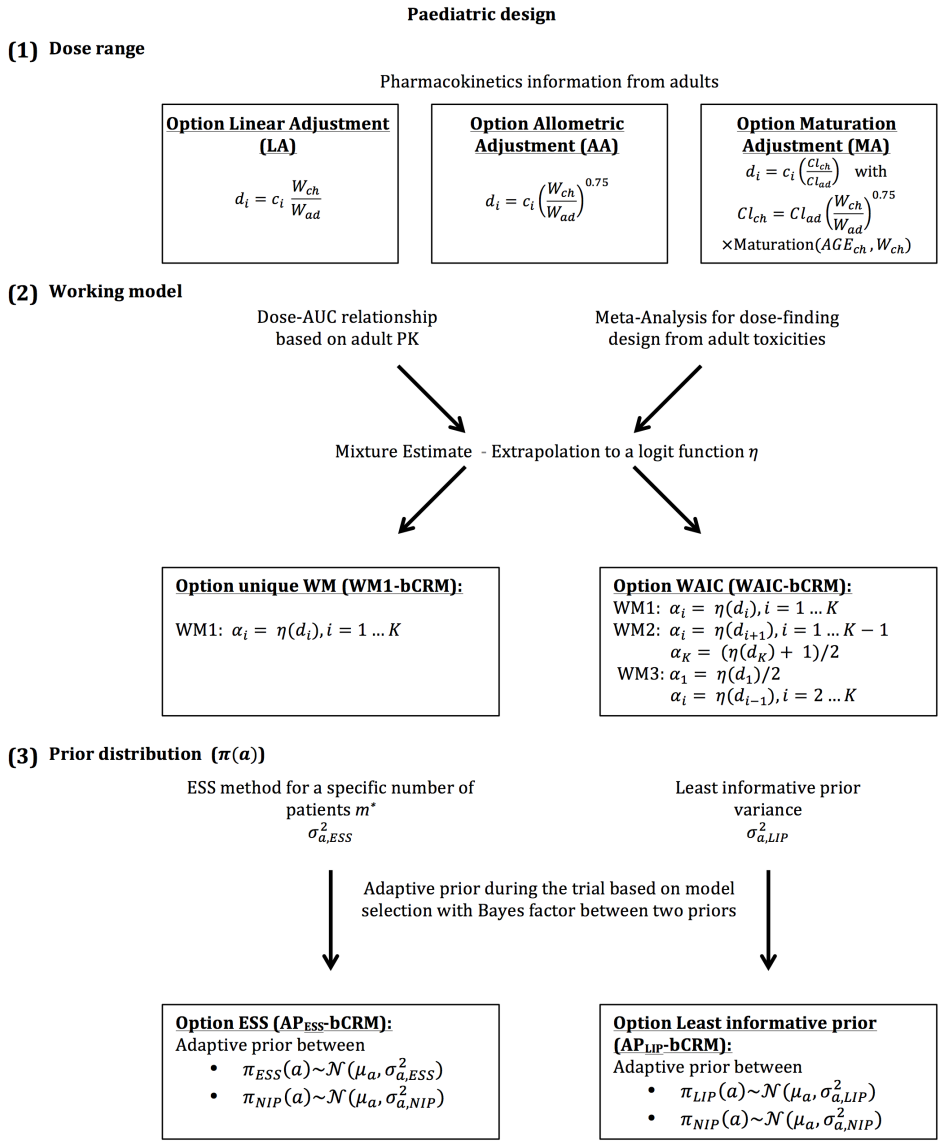


Figure 1. General framework describing the different proposed steps in the planification of paediatric dose-finding clinical trials. It is composed of (1) the choice of the dose-range with three different possible options, linear adjustment (LA), allometric adjustment (AA) and maturation adjustment (MA). They are built using extrapolation from adults to children, with d_i the paediatric dose, c_i the adult dose and W_{ch} and W_{ad} respectively the children and adult weight; (2) the working model (WM) specification, where adult PK and toxicities can be used to build a toxicity function η . It allows to calculate the WMs ($\alpha_i, i \in 1, \dots, K$) for each dose i ; and (3) the specification of the prior density parameter $a, \pi(a)$, of the dose-reponse relationship.

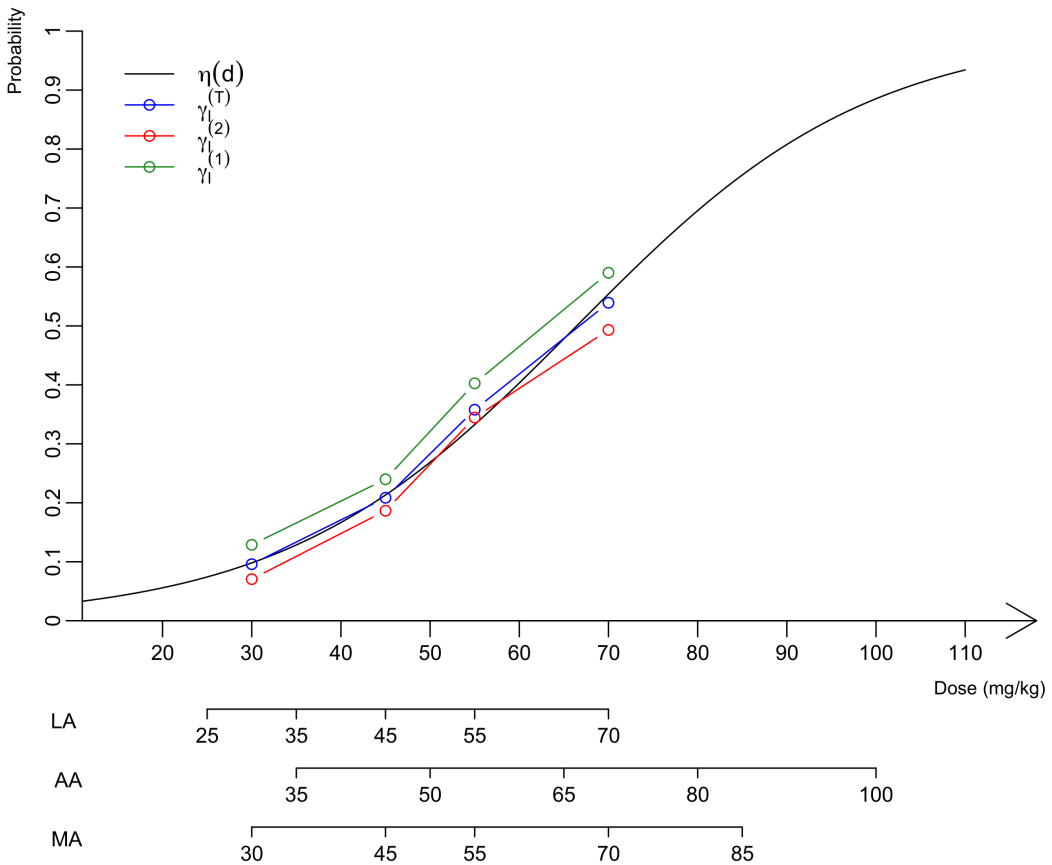


Figure 2. Representation of the estimated probabilities of toxicity used to build WMs for paediatrics according to dose (mg/kg). The logit function $\eta(d)$ in black fits the estimated dose-toxicity relationship, $\gamma_{\ell}^{(T)}$ ($\ell = 1, 2, 3, 4$), in blue, which is the mixture of both estimated dose-toxicity curves, $\gamma_{\ell}^{(1)}$, based on adult PK information, in green, and $\gamma_{\ell}^{(2)}$, based on adult phase I observations, in red. The different dose-range for the LA, AA and MA options are represented below the graph.

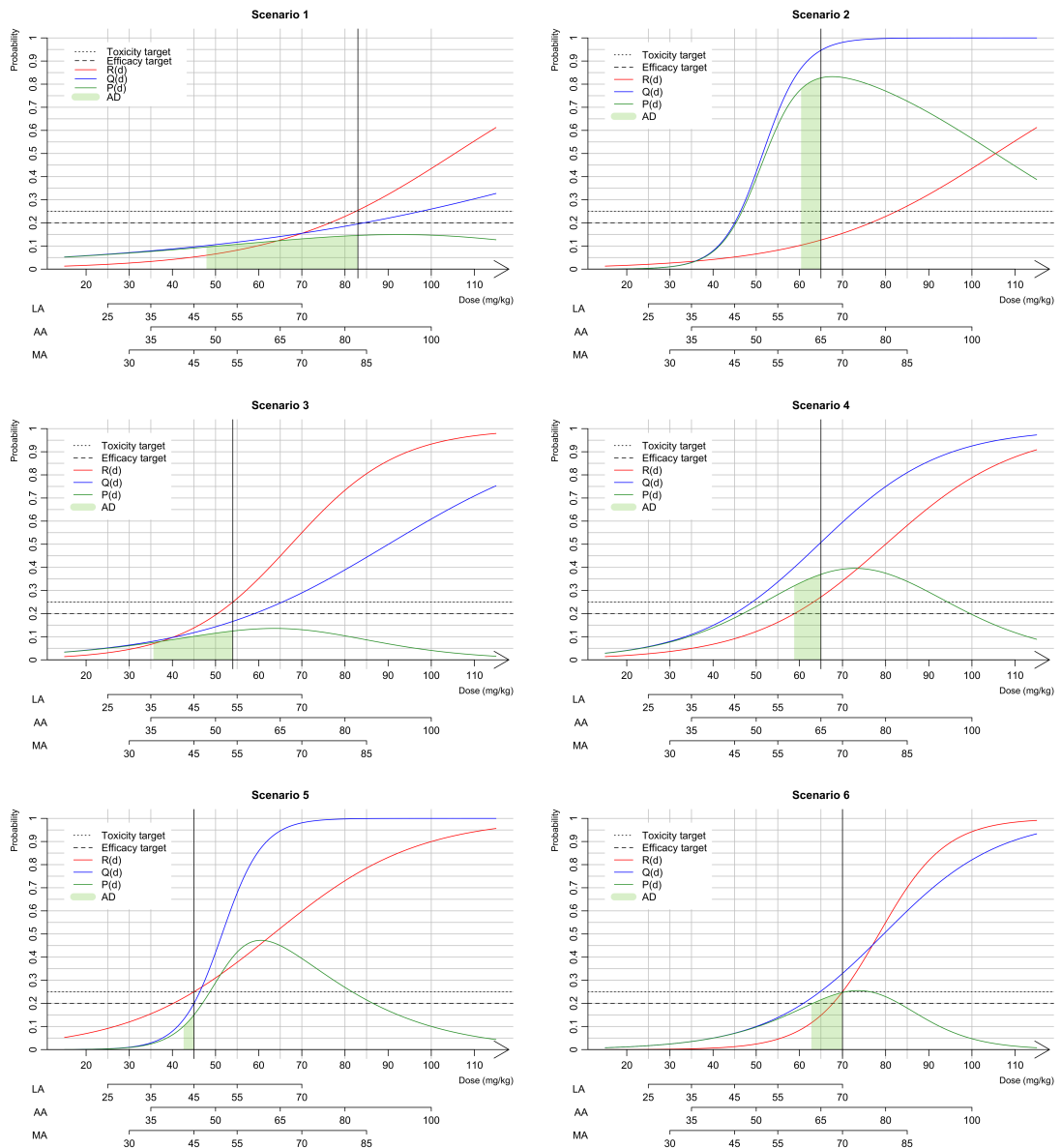


Figure 3. Presentation of the six scenarios used in the simulation study. The dose-toxicity, $R(d)$, curve is in red, the dose-efficacy, $Q(d)$, curve is in blue and the dose-success, $P(d)$, curve is in green. The sMSD is represented by black vertical line, the toxicity and efficacy targets are given with dashed lines. The admissible doses (AD) are given by the green area under the success $P(d)$ curve.